

## 13ème Colloque National en Calcul des Structures

### Multistable shell structures satisfying clamped boundary conditions: An analysis by the polar method

M. Brunetti<sup>1</sup>, A. Vincenti<sup>2</sup>, S. Vidoli<sup>3</sup>

<sup>1</sup> Dipartimento di Chimica Materiali Ambiente, Sapienza Università di Roma, [matteo.brunetti@uniroma1.it](mailto:matteo.brunetti@uniroma1.it)

<sup>2</sup> Institut Jean Le Rond d'Alembert, Sorbonne Universities, UPMC Univ Paris06, [angela.vincenti@upmc.fr](mailto:angela.vincenti@upmc.fr)

<sup>3</sup> Dipartimento di Ingegneria Strutturale e Geotecnica, Sapienza Università di Roma, [stefano.vidoli@uniroma1.it](mailto:stefano.vidoli@uniroma1.it)

---

**Résumé** — Multi-stable shells have been recently proposed as an effective solution to design morphing structures. We describe a class of shallow shells which are bistable after one of their sides is completely clamped. Employing the polar method, we investigate the influence of the constitutive properties of the laminate on its multistability.

**Mots clés** — Morphing Structures, Multistability, Bistable clamped shells, Polar method.

---

## 1 Introduction

One of the emerging challenges in structural engineering is to design structures able to face quite different operating conditions. This goal can be achieved by resorting to morphing structures. Roughly speaking, it can be said *morphing* a structure or a structural system capable of updating its geometric configuration in order to satisfy some performance requirements. Even if morphing structures are spreading in some areas of structural engineering (see [4]), much remains to be done to properly design and implement this kind of systems.

Morphing structures can be realized by means of multistable shells. A multistable shell is merely an *elastic surface* that exhibit more than one equilibrium configuration, even without applied external actions. Since actuation is required only to switch between the alternative stable states and it can be realized with a limited actuation force (e.g., by triggering instability phenomena, or by exploiting displacement amplifications due to geometrical nonlinearities), multistable shells turn out to be a cheap way to get structural systems capable of considerable shape change.

Multistability in shells stems from a complex interplay between geometric nonlinearities and elastic properties and it can be achieved in various ways including pre-stresses, initial curvatures and plastic deformations. Moreover, multistability is highly sensitive to boundary conditions. The *global stability scenario* (the number of the stable equilibrium configurations, their shapes and their 'robustness') depends on such choices and should be known to properly design the morphing system. However stable states usually have quite different shape and the transition between them may be realized by several load paths : to depict such global stability scenario Finite Element analysis serve little purpose and *reduced* shell models with few degrees of freedom are required.

For shallow shells, as the ones commonly used in technological applications, the nonlinear (generalized) von Kármán shell model [20] can be chosen as 'parent' model. Then, the discrete model can be generated by reducing the parent model to a low-dimensional subspace by means of a careful selection of admissible configurations. Indeed, in order to be effective the reduction should globally preserve the multi-well elastic energy of the parent model [13, 18, 19].

To the best of the authors knowledge most of the literature studies deal with shells completely free on their sides, see for instance [3, 5, 6, 10, 12, 13, 18]. Despite the relevance of boundary conditions, only few works address the design of multistable constrained shells [7, 11]. In [1] the authors used the reduction procedure proposed in [19] to infer a three-degrees-of-freedom reduced model capable of predicting the multistable behavior of pseudo-conical cantilever orthotropic shells. They identify two

compact disjoint regions in the plane of shell initial curvatures corresponding to shells bistable *after clamping*, thus opening the way to a more general approach to design and optimization of multistable shells.

In this contribution the same model is used to investigate how the material elastic constants affect the multistability of clamped shells. To this aim, we employ the *polar method* [17] which makes it possible to express the elasticity tensor of an anisotropic material in terms of its invariant quantities. Here, the initial geometry of the natural stress-free configuration of the shell and the constitutive properties are the primary means to induce bistability : we do not consider other sources of multistability (e.g., inelastic pre-stresses, see [8]). For sake of simplicity we chose two initial geometry for the shell natural configuration and we consider uncoupled quasi-homogeneous orthotropic laminates [15]. We detect the regions in the plane of the polar moduli corresponding to shells which turn out to be bistable after clamping ; moreover, we investigate the influence of the polar moduli on the shape of the clamped stable configurations.

## 2 Design parameters

### 2.1 Natural shape

We consider shallow shells with pseudo-conic natural configurations described by surfaces in the form :

$$S_0 = \{(x, y, w_0(x, y)), 0 \leq x \leq L_x, -L_y/2 \leq y \leq L_y/2\},$$

with :

$$w_0(x, y) = \frac{y^2}{2} \left( h_1 + (h_2 - h_1) \frac{x}{L_x} \right), \quad (1)$$

for some  $h_1, h_2 \in \mathbb{R}$  and  $0 < L_y \leq L_x$ . The geometry of the natural configuration of the shell is completely defined by three design parameters : the aspect ratio  $\eta = L_x/L_y \geq 1$  and the real numbers  $h_1$  and  $h_2$ , which measure the curvatures of the edges parallel to the  $y$ -direction  $x = 0$  and  $x = L_x$ , respectively. In what follows two different initial configurations are considered, see Figure 2.1. The corresponding

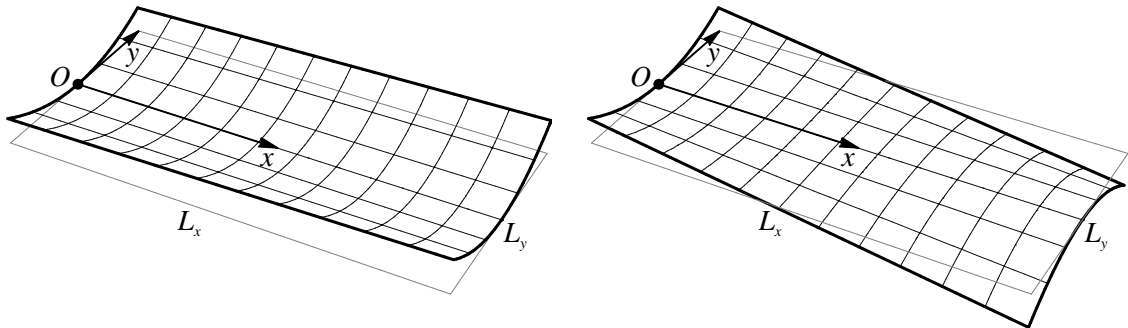


FIGURE 1 – Natural configurations of the shell. Left : first shell (*quasi-cylindrical*) ; Right : second shell.

values for the design parameters are listed in Table 1. The curvatures  $h_1, h_2$  have been chosen so that the shallowness ratio  $w_{max}/L_y$  is  $1/8$  for the edge  $x = 0$  to clamp,  $1/6$  for the edge  $x = L_x$  to leave free. The two shells only differ by the sign of the curvature of the free edge. Since curvatures are only slightly different, we will call the first shell *quasi-cylindrical*.

TABLE 1 – Geometric design parameters

	$L_x$	$L_y$	$h_1$	$h_2$
	m	m	1/m	1/m
First shell ( <i>quasi-cylindrical</i> shell)	0.3	0.15	1/0.15	1/0.1125
Second shell	0.3	0.15	1/0.15	-1/0.1125

## 2.2 Material constants

In Voigt notation, let us denote with :  $\underline{M} = \{M_x, M_y, M_{xy}\}$  the bending moments ;  $\underline{N} = \{N_x, N_y, N_{xy}\}$  the membrane stresses ;  $\underline{k} = \{k_x, k_y, 2k_{xy}\}$  the curvatures ;  $\underline{e} = \{e_x, e_y, 2e_{xy}\}$  the membrane strains. Moreover, let  $\underline{f} = \{f_x, f_y, 2f_{xy}\}$  represent non-zero membrane stresses in the flat reference configuration, and curvatures  $\underline{h} = \{h_x, h_y, 2h_{xy}\}$  provide non-zero bending moments in the reference configuration. Since we do not consider inelastic pre-stresses, the Gauss compatibility equation holds true :

$$\frac{\partial^2 f_x}{\partial y^2} + \frac{\partial^2 f_y}{\partial x^2} - 2 \frac{\partial^2 f_{xy}}{\partial x \partial y} = h_y h_x - h_{xy}^2$$

For an uncoupled orthotropic shell, we assume the principal material directions aligned with the coordinate directions  $x$  and  $y$ . Then, the constitutive relations between bending moments and curvatures  $\underline{M} = \underline{D} \underline{k}$  read as :

$$\begin{aligned} M_x &= D_{11}(k_x - h_x) + D_{12}(k_y - h_y), & M_{xy} &= D_{33}(k_{xy} - h_{xy}), \\ M_y &= D_{12}(k_x - h_x) + D_{22}(k_y - h_y), \end{aligned} \quad (2)$$

The relations between membranal stresses and membranal strains  $\underline{N} = \underline{A} \underline{e}$  will read as :

$$\begin{aligned} N_x &= A_{11}(e_x - f_x) + A_{12}(e_y - f_y), & N_{xy} &= A_{33}(e_{xy} - f_{xy}), \\ N_y &= A_{12}(e_x - f_x) + A_{22}(e_y - f_y), \end{aligned} \quad (3)$$

Moreover we suppose the shells to be quasi-homogeneous [15], i.e., we consider laminates having the same elastic behaviour in tension and bending in each direction ; for  $t$  the shell thickness this implies

$$\underline{D} = \frac{t^2}{12} \underline{A}, \quad \underline{A}/A_{11} = \underline{D}/D_{11} = \begin{bmatrix} 1 & \nu & 0 \\ \nu & \beta & 0 \\ 0 & 0 & \gamma \end{bmatrix}$$

Here :  $\beta = D_{22}/D_{11} = A_{22}/A_{11}$  is the ratio between the membrane and bending stiffnesses in the coordinate directions,  $\gamma = D_{33}/D_{11} = A_{33}/A_{11}$  is the shear and torsional moduli and  $\nu = D_{12}/D_{11} = A_{12}/A_{11}$  is the in-plane and out-of-plane Poisson effects. By employing the polar method we express the dimensionless constitutive parameters  $\beta$ ,  $\nu$ ,  $\gamma$  in terms of the invariants of the elasticity tensors, say the polar moduli. For laminates with identical layers it can be shown that the isotropic parts of the homogenised elastic tensors  $(12/t^3)\underline{D} = \underline{A}/t$  are equal and coincide to that of the elementary layer, say  $T_0^\ell, T_1^\ell$ . As a consequence  $\beta$ ,  $\nu$ ,  $\gamma$  only depend on two polar moduli, say  $R_0^k = (-1)^k R_0$ , with  $k \in \{0, 1\}$ , and  $R_1$ , which measure the anisotropic part of the elastic tensors :

$$\begin{aligned} \beta(R_0^k, R_1) &= \frac{T_0^\ell + 2T_1^\ell + R_0^k + 4R_1}{T_0^\ell + 2T_1^\ell + R_0^k + 4R_1}, & \nu(R_0^k, R_1) &= \frac{-T_0^\ell + 2T_1^\ell - R_0^k}{T_0^\ell + 2T_1^\ell + R_0^k + 4R_1} \\ \gamma(R_0^k, R_1) &= \frac{T_0^\ell - R_0^k}{T_0^\ell + 2T_1^\ell + R_0^k + 4R_1} \end{aligned}$$

For the elastic tensors to be positive definite some restrictions on the polar moduli shall be considered, leading to an admissible *elastic* domain in the plane  $R_0^k - R_1$ . However, for laminates tailored by bonding together identical plies some more restrictive *geometric* bounds arise from the combination of the layer orientations and position in the stack, see [16]. In our case, such admissible domain is defined by the conditions, see Figure 2 :

$$R_0 - R_0^\ell \left[ 2 \left( \frac{R_1}{R_1^\ell} \right)^2 - 1 \right] \geq 0, \quad -R_0^\ell \leq R_0^k \leq R_0^\ell, \quad -R_1^\ell \leq R_1 \leq R_1^\ell$$

Shells represented by a lamination point on the curved boundary of the domain are made by *angle-ply* laminates, i.e., laminates composed by an even number of plies and having for each ply at the orientation  $\theta$  a ply at the orientation  $-\theta$ . As an example, point  $B$  of Figure 2 corresponds to  $\theta = 45^\circ$  : the shells studied in [1] belong to this class of laminates. The straight line between the two points  $A$  and  $C$  represents

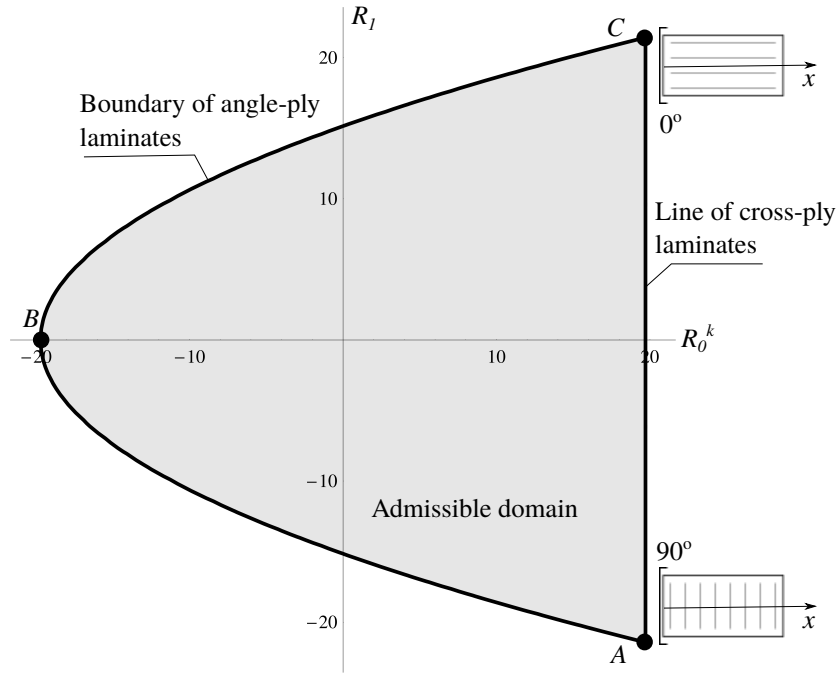


FIGURE 2 – Admissible domain in the plane of the polar moduli. Values are in GPa.

*cross-ply* laminates, i.e., laminates having layers at  $0^\circ$  or  $90^\circ$ , in relative quantities depending upon the location of the lamination point on the line. By simplifying, moving from  $A$  to  $C$  the stiffness in the  $x$ -direction increases while the stiffness in the  $y$ -direction decreases. In what follows we chose the polar moduli  $R_0^k$  and  $R_1$  as design parameters. For each of the shell natural configurations we consider, we want to determine the regions in the plane  $R_0^k - R_1$  corresponding to shells bistable after clamping. To perform the numerical analysis, an highly anisotropic unidirectional carbon/epoxy ply (T300/5208) (see [14], [9]) has been chosen ; technical moduli and polar parameters are listed in Table 2.

TABLE 2 – Material properties unidirectional carbon/epoxy ply (T300/5208).

$E_1$	$E_2$	$\nu_{12}$	$G_{12}$	$T_0^\ell$	$T_1^\ell$	$R_0^\ell$	$R_1^\ell$
GPa	GPa	-	GPa	GPa	GPa	GPa	GPa
181	10.3	0.28	7.17	26.9	24.7	19.7	21.4

### 3 Reduced nonlinear model

For shells having the natural shapes described by (1), we examine the stability properties once the side  $x = 0$  has been clamped. We want to characterize the number and the nature of all stable equilibria.

#### 3.1 Modelling assumptions

We briefly recall the main assumptions of the generalized von-Kármán (FvK), see [2] for details. We shall consider shell configurations in the form :

$$\mathcal{S} = \{(x + u(x, y), y + v(x, y), w(x, y)), 0 \leq x \leq L_x, -L_y/2 \leq y \leq L_y/2\},$$

where the in-plane displacement fields  $u$  and  $v$  and the transverse displacement field  $w$  scale as :  $u, v = O(\varepsilon^2)$ ,  $w = O(\varepsilon)$ , with  $\varepsilon = t^2/R^2$  a small parameter,  $R$  being the characteristic radius of curvature of the shell. By assuming these scaling laws, the contributions of the in-plane and transverse displacements to

the membrane strains of the surface  $\mathcal{S}$  are comparable, so that we have :

$$e_x = \frac{\partial u}{\partial x} + \frac{1}{2} \left( \frac{\partial w}{\partial x} \right)^2, \quad e_y = \frac{\partial v}{\partial y} + \frac{1}{2} \left( \frac{\partial w}{\partial y} \right)^2, \quad e_{xy} = \frac{1}{2} \left( \frac{\partial v}{\partial x} + \frac{\partial u}{\partial y} + \frac{\partial w}{\partial x} \frac{\partial w}{\partial y} \right) \quad (4)$$

Instead the curvatures of the surface  $\mathcal{S}$  only depend on the transverse displacement :

$$k_x = \frac{\partial^2 w}{\partial x^2}, \quad k_y = \frac{\partial^2 w}{\partial y^2}, \quad k_{xy} = \frac{\partial^2 w}{\partial x \partial y} \quad (5)$$

The stable equilibria of a FvK shell are the local minima of the total energy, sum of the bending and membrane contribution :

$$\mathcal{E}(u, v, w) = \frac{1}{2} \int_0^{L_x} \int_{-L_y/2}^{L_y/2} (M_x k_x + M_y k_y + 2M_{xy} k_{xy}) dA + \frac{1}{2} \int_0^{L_x} \int_{-L_y/2}^{L_y/2} (N_x e_x + N_y e_y + 2N_{xy} e_{xy}) dA, \quad (6)$$

with the bending moments and membrane stresses as in (2) and (3). We observe that the in-plane displacement field can be computed in terms of the transverse displacement solving a linear elasticity problem. This allows us to use an effective minimization strategy for the (6). Indeed, necessary conditions for the functional  $\mathcal{E}$  to be stationary with respect to  $u$  and  $v$  are :

$$\frac{\partial N_x}{\partial x} + \frac{\partial N_{xy}}{\partial y} = 0, \quad \frac{\partial N_{xy}}{\partial x} + \frac{\partial N_y}{\partial y} = 0$$

while for the system (4) and (5) to be integrable the Gauss compatibility condition holds true :

$$\frac{\partial^2 e_x}{\partial y^2} + \frac{\partial^2 e_y}{\partial x^2} - 2 \frac{\partial^2 e_{xy}}{\partial x \partial y} = k_x k_y - k_{xy}^2. \quad (7)$$

By inversion of the constitutive relations (3), (7) is transformed in terms of stresses to get a standard plane elasticity problem which is linear in the data, namely the difference in gaussian curvature between the actual and natural configurations,  $\Delta g = \det k - \det h$  (see [19], [1]). As we will point out, the linearity of the membrane problem plays a crucial role in the reduction procedure used to deduce a discrete approximation with few degrees of freedom of the FvK functional (6).

### 3.2 Reduction procedure

We summarize the main steps of the reduction procedure (see [19], [1] for details).

*Step 1.* We introduce an ansatz for the transverse displacement field. Here we seek  $w$  in the form

$$w(x, y) = q_1 \frac{x^2}{2} + q_2 \frac{y^2}{2} + q_3 \frac{x^3}{6} + q_4 \frac{x^2 y^2}{2} + q_5 \frac{xy^2}{2}, \quad (8)$$

so that it is uniquely defined by five Lagrangian parameters  $q_1$  to  $q_5$ . We remark that the assumption (8) shall include the pseudo-conical natural configurations. Moreover, (8) allows to easily handle the clamp boundary condition on the edge  $x = 0$ . Indeed, one easily obtains  $q_2 = 0, q_5 = 0$ . Therefore, the clamped shell has only three degrees of freedom.

*Step 2.* We compute the forcing term of the linear membrane problem  $\Delta g$ . For shells constrained by the clamp condition, using (5) and (8) we have

$$k_x = q_1 + q_3 x + q_4 y^2, \quad k_y = q_4 x^2, \quad k_{xy} = q_4 xy,$$

so that

$$\Delta g = q_1 q_4 x^2 + q_3 q_4 x^3 + \frac{(h_1 - h_2)^2}{L_x^2} y^2 - 3 q_4^2 x^2 y^2. \quad (9)$$

*Step 3.* We solve the linear membrane problem for  $\Delta g$  given by (9). Due to the linearity of the differential problem, we have to solve the same problem for all the following four forcing terms  $\{x^2, x^3, y^2, x^2 y^2\} \rightarrow \{N^{20}, N^{30}, N^{02}, N^{22}\}$ . Then, we use the same linear combination as in (9) to compute the membrane stress field

$$\underline{N} = q_1 q_4 \underline{N}^{20} + q_3 q_4 \underline{N}^{30} + \frac{(h_1 - h_2)^2}{L_x^2} \underline{N}^{02} - 3 q_4^2 \underline{N}^{22} \quad (10)$$

The auxiliary membrane problems can be solved with standard Finite element codes. We remark that the high precision we can achieve in this way turns out to be the key ingredient of the procedure ; Indeed it ensures a good estimate of the membrane energy, which is the dominant term of the elastic energy functional.

*Step 4.* We use the ansatz for the transverse displacement (8) and the computed membrane stress solution (10) to get the energy functional (6) as function of the Lagrangian parameters  $\mathcal{E} \simeq \hat{\mathcal{E}}(q_1, q_3, q_4)$ . As the membrane stresses (10) and strains, through (3), are second-order polynomials of  $q_1, q_3, q_4$ , the approximated functional  $\hat{\mathcal{E}}(q_1, q_3, q_4)$  is a fourth-order polynomial in the Lagrangian parameters.

## 4 Results

Figure 3 displays the global stability scenario in the plane of the polar moduli. Within the admissible

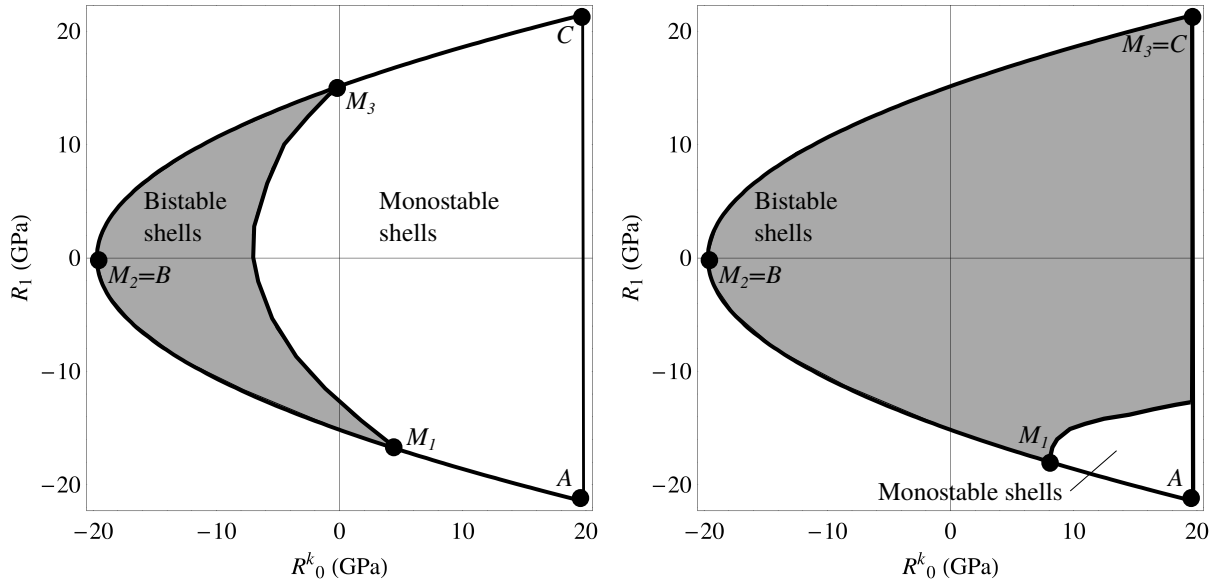


FIGURE 3 – Stability scenario in the plane of polar moduli. Left : quasi-cylindrical shell. Right : pseudo-conical shell.

domain, shells corresponding to gray points are *bistable* after clamping while shells corresponding to white points turn out to be *monostable* when clamped. Not surprisingly, the bistable region is wider for the second shell ; indeed, cylindrical shells are proved to be close to the margin of bistability region, see [1]. We focus on three points on the boundary of angle-ply laminates,  $M_1, M_2, M_3$ , see Figure 3. In both cases,  $M_1$  and  $M_3$  are found as the intersections with the boundary of the monostability region ;  $M_2$  corresponds to the  $\pm 45^\circ$  laminate previously studied in [1]. Since all of these points lie on the bistability region, at each of them correspond *two* clamped stable configurations. As noted above, moving from  $A$  to  $C$ , and then also from  $M_1$  to  $M_3$ , the stiffness in the  $x$ -direction increases while the stiffness in the  $y$ -direction decreases. We investigate the shape of the clamped stable configurations by computing the curvatures  $K_x = k_x(L_x/2, 0)/2$  and  $K_y = k_y(L_x)$ . Moreover we plot the energy profile computed on the straight line joining the minima.

*First shell (Pseudo-cylindrical shell).* Moving from  $M_1$  to  $M_3$  we observe a sharp reduction of the curvature  $K_x$  of the minimum which lose its stability. Moreover, the two stable configurations tend to coalesce, see Figure 4. This reduction sounds mechanically reasonable as the stiffness in the  $x$ -direction is increasing. Furthermore, passing from  $M_1$  to  $M_3$ , even the elastic energy stored after the clamping is strongly reduced. This is because it is becoming lower and lower the stiffness in the direction parallel to the edge which is to be clamped.

*Second Shell.* Even in this case, moving from  $M_1$  to  $M_3$  we observe a sharp reduction of the curvature  $K_x$  for the minimum which lose its stability, see Figure 5. Moreover, as in the previous case, moving from  $M_1$  to  $M_3$ , the minimum which survives suffers only a slight change in its shape and the elastic energy stored after the clamping is strongly reduced. However, in this case the different sign of the natural curvatures  $h_1, h_2$  forces the other minimum to have an *S-shaped* configuration for high values of the

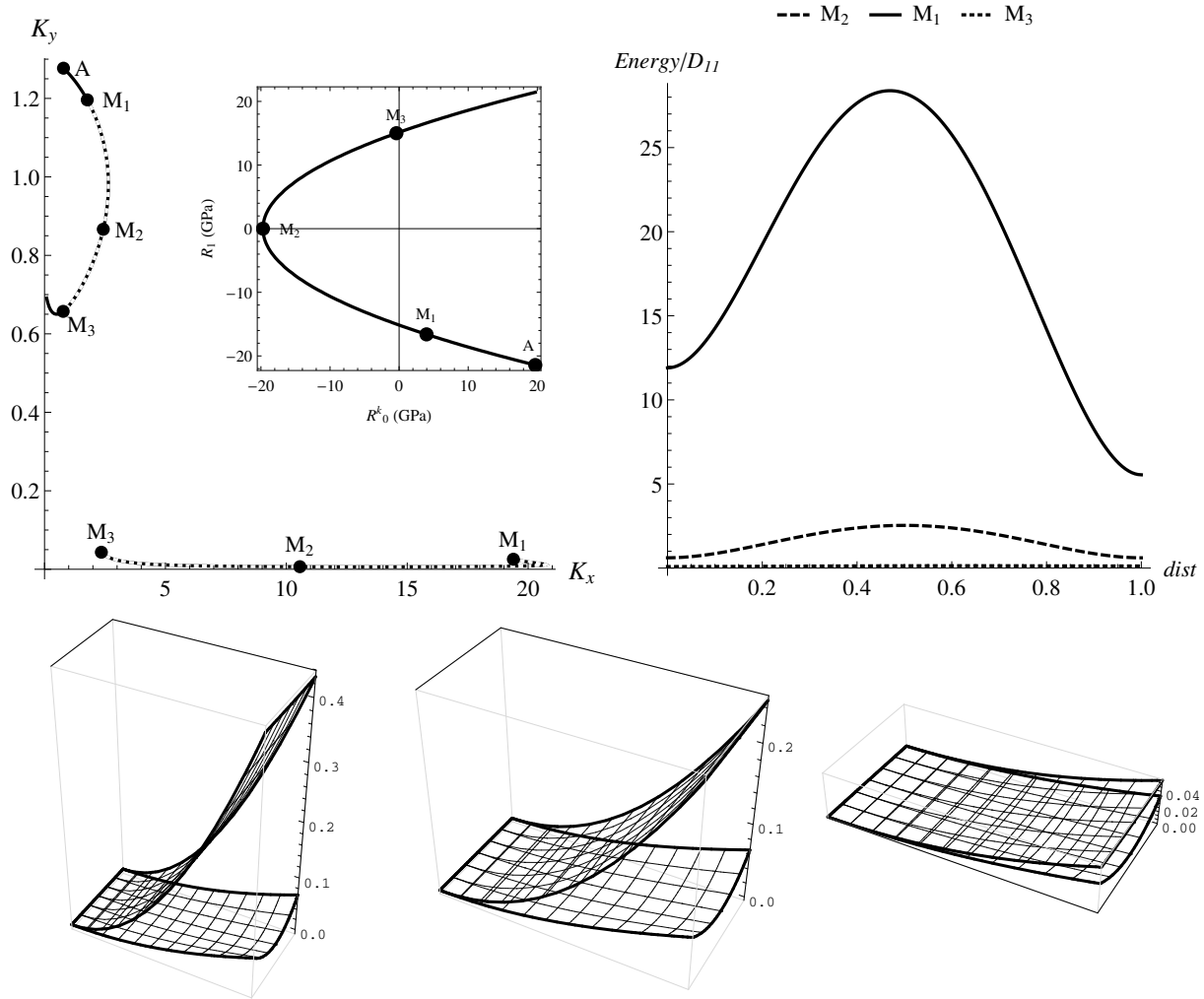


FIGURE 4 – First shell (quasi-cylindrical shell).

stiffness in the  $y$ -direction ( $M_1$  point). For low values of the stiffness in the  $y$ -direction the free edge changes its concavity ( $M_3$  point) so that the curvature  $K_y$  of the clamped stable configuration and the curvature  $h_2$  of the natural configuration have different signs.

## Références

- [1] M Brunetti, A Vincenti and S Vidoli. A class of morphing shell structures satisfying clamped boundary conditions *International Journal of Solids and Structures*, 82 :47 – 55, 2016.
- [2] P G Ciarlet. A justification of the von Kármán equations. *Archive for Rational Mechanics and Analysis*, 73 :349–389, 1980.
- [3] B H Coburn, A Pirrera, P M Weaver, and S Vidoli. Tristability of an orthotropic doubly curved shell. *Composite Structures*, 96 :446–454, 2013.
- [4] S Daynes, P M Weaver, and J A Trevarthen. A morphing composite air inlet with multiple stable shapes. *Journal of Intelligent Material Systems and Structures*, 22(9) :961–973, 2011.
- [5] A Fernandes, C Maurini, and S Vidoli. Multiparameter actuation for shape control of bistable composite plates. *International Journal of Solids and Structures*, 47(10) :1449–1458, 2010.
- [6] E Lamacchia, A Pirrera, I V Chenchiah, and P M Weaver. *Morphing shell structures : A generalised modelling approach*. *Composite Structures*, 131 :1017-1027, 2015.
- [7] F Mattioni, P M Weaver and M I Friswell. *Multistable composite plates with piecewise variation of lay-up in the planform*. *International Journal of Solids and Structures*, 46(1) :151-164, 2009.
- [8] W Hamouche, C Maurini, A Vincenti, and S Vidoli. Simple recipes to design and produce multistable shells. *Meccanica*, submitted.

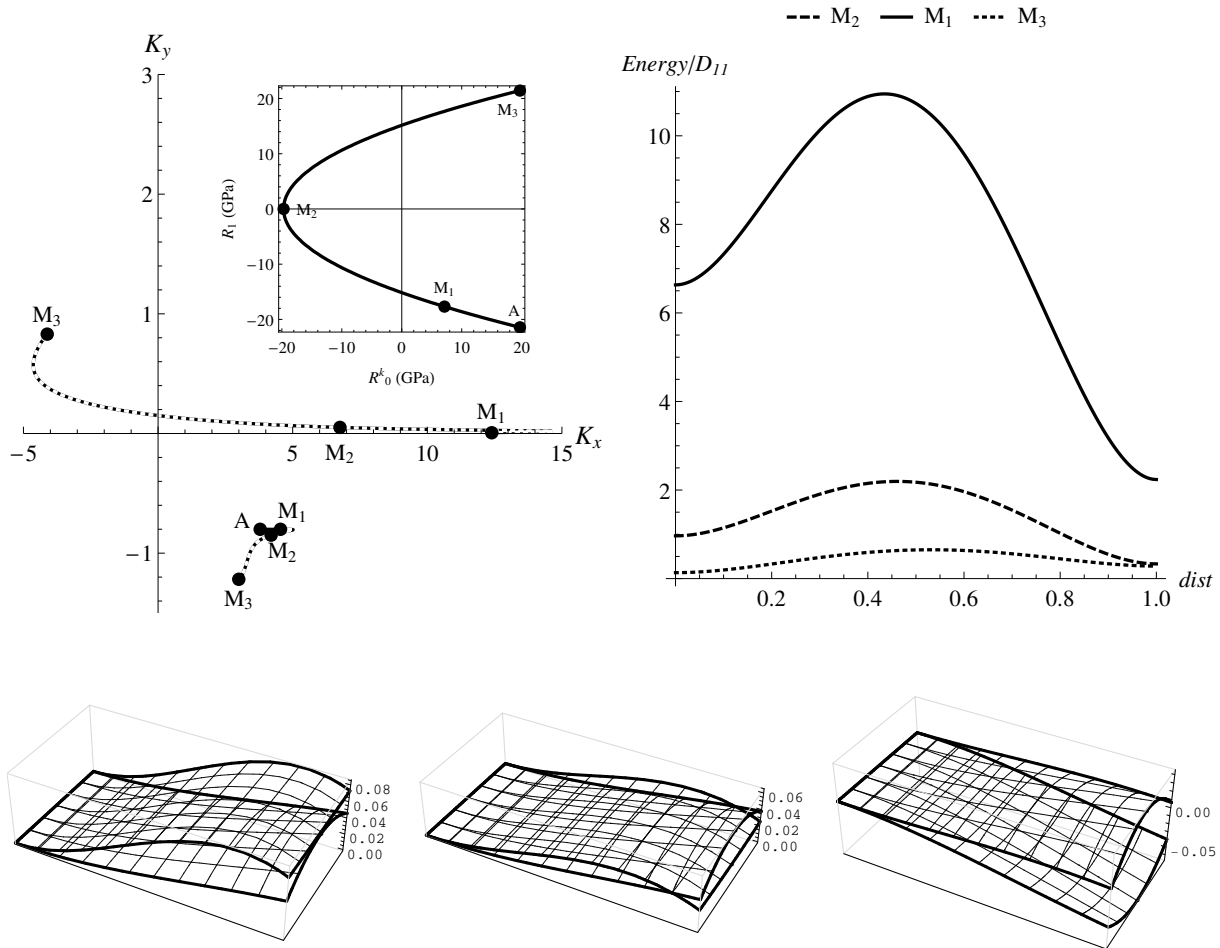


FIGURE 5 – Second shell.

- [9] M Montemurro, A Vincenti and P Vannucci. *Design of the elastic properties of laminates with a minimum number of plies..* Mechanics of Composite Materials, 48(4) :369-390, 2012.
- [10] A D Norman, K A Seffen, and S D Guest. Multistable corrugated shells. *Proceedings of the Royal Society of London A : Mathematical, Physical and Engineering Sciences*, Vol. 464(2095) :1653-1672, 2008.
- [11] A S Panesar and P M Weaver. Optimisation of blended bistable laminates for a morphing flap. *Composite Structures*, 94(10), 3092-3105, 2012.
- [12] A Pirrera, D Avitabile, and P M Weaver. On the thermally induced bistability of composite cylindrical shells for morphing structures. *International Journal of Solids and Structures*, 49(5) :685–700, 2012.
- [13] K A Seffen. Morphing bistable orthotropic elliptical shallow shells. *Proceedings of the Royal Society A : Mathematical, Physical and Engineering Science*, 463(2077) :67–83, 2007.
- [14] S W Tsai and T Hahn. Introduction to composite materials. *Technomic*, 1980
- [15] P Vannucci and G Verchery. A special class of uncoupled and quasi-homogeneous laminates. *Composites Science and Technology*, 61(10) :1465 – 1473, 2001.
- [16] P Vannucci. A note on the elastic and geometric bounds for composite laminates. *Journal of Elasticity*, 112(2) :199 – 215, 2013.
- [17] G Verchery. Les invariants des tenseurs d’ordre 4 du type de l’élasticité. *Mechanical Behavior of Anisotropic Solids/Comportement Mécanique des Solides Anisotropes*, 93 – 104, 1982.
- [18] S Vidoli and C Maurini. Tristability of thin orthotropic shells with uniform initial curvature. *Proceedings of the Royal Society A : Mathematical, Physical and Engineering Science*, 464(2099) :2949–2966, 2008.
- [19] S Vidoli. Discrete approximations of the Föppl - von Kármán shell model : From coarse to more refined models. *International Journal of Solids and Structures*, 50(9) :1241 – 1252, 2013.
- [20] T Von Kármán. *Festigkeitsprobleme im maschinenbau*. Encyklopädie der Mathematischen Wissenschaften. 1910.